International Journal of Environmental Technology and Management

ISSN online: 1741-511X - ISSN print: 1466-2132
https://www.inderscience.com/ijetm

A drought monitoring method in the Yellow River basin based on boundary extraction of remote sensing images

Yang Liu, Xiaodong Shi, Ge Zhang, Shaofeng Zhao, Ze Wang

DOI: 10.1504/IJETM.2023.10053933

Article History:

Received:	27 July 2022
Last revised:	01 September 2022
Accepted:	07 December 2022
Published online:	18 December 2023

A drought monitoring method in the Yellow River basin based on boundary extraction of remote sensing images

Yang Liu, Xiaodong Shi, Ge Zhang* and Shaofeng Zhao

Cloud Computing and Big Data Institute,
Henan University of Economics and Law,
Zhengzhou Henan, 450046, China
Email: liuyang@huel.edu.cn
Email: sxd@huel.edu.cn
Email: zg@huel.edu.cn
Email: zsf@huel.edu.cn
*Corresponding author

Ze Wang

College of Electrical Engineering and Information Engineering,
Lanzhou University of Technology,
Lanzhou Gansu, 730050, China
Email: wz0602@hotmail.com

Abstract: In order to improve the extraction accuracy of remote sensing image boundary information and improve the fitting degree between drought monitoring results and actual results, this study designed a drought monitoring method in the Yellow River basin based on boundary extraction of remote sensing images. ETM+ Landsat satellite was selected to collect real-time remote sensing images comprehensively. After geometric correction and radiometric correction, edge information is extracted from remote sensing image data. Then the spatial inversion process of remote sensing index and surface temperature characteristics is established, and the drought monitoring level of the Yellow River basin is set after the elevation correction. According to the experiment, the accuracy of the method to extract the image boundary information is always above 91.7%, and the fitting degree between the obtained drought monitoring results and the actual results is always above 0.94, indicating that the method effectively achieves the design expectation.

Keywords: Yellow River basin; drought conditions; remote sensing monitoring; remote sensing image; boundary extraction.

Reference to this paper should be made as follows: Liu, Y., Shi, X., Zhang, G., Zhao, S. and Wang, Z. (2024) 'A drought monitoring method in the Yellow River basin based on boundary extraction of remote sensing images', *Int. J. Environmental Technology and Management*, Vol. 27, Nos. 1/2, pp.23–36.

Biographical notes: Yang Liu received his BS and MS in Computer Science and Technology from the Zhengzhou University, Zhengzhou, China, in 2003 and 2006, respectively, and PhD in Computer Architecture from the Huazhong

University of Science and Technology, Wuhan, China in 2013. He is currently an Associate Professor at the Cloud Computing and Big Data Institute of Henan University of Economics and Law, Zhengzhou, China. His research interests include massive storage system, data mining and machine learning. He has published 26 research articles, three of which was indexed by SCI and nine by EI. Besides, he has hosted or participated in 16 research projects.

Xiaodong Shi received his MS degree from the Zhengzhou University, Zhengzhou, China, in 2006, and PhD degree from the School of Computer Science and Technology, HuaZhong University of Science and Technology, Wuhan, China, in 2012. He is currently an Associate Professor at the School of E-Commerce and Logistics Management of Henan University of Economics and Law, Zhengzhou, China. His research interests include deep learning, evolutionary optimisation and big data mining. He has published 12 research articles, five of which was indexed by SCI or EI. Besides, he has hosted or participated in 11 research projects.

Ge Zhang received her BS in Computer Science and Technology from the Zhengzhou University, Zhengzhou, China, in 2011 and MS in Computer Science and Technology from the Beijing University of Technology, Beijing, China in 2015. She is currently a Lecturer at the Cloud Computing and Big Data Institute of Henan University of Economics and Law, Zhengzhou, China. Her research interests include data mining and machine learning. She has published 12 research articles, three of which was indexed by EI. Besides, she has participated in nine research projects.

Shaofeng Zhao received his BS and MS in Computer Science and Technology from the Zhengzhou University, Zhengzhou, China, in 2008 and 2013, respectively. He is studying for a Doctor's degree in Computer Architecture from the Huazhong University of Science and Technology, Wuhan, China. He is currently an instructor at the Cyberspace Administration Centre of Henan University of Economics and Law, Zhengzhou, China. His research interests include next-generation memory technologies and machine learning. He has published six research articles, five of which were indexed by SCI and EI. Besides, he has hosted or participated in nine research projects.

Ze Wang received his BS in Electrical Engineering and Automation from the Hubei University of Technology, Wuhan, China, in 2019. He is currently studying for his MS degree in the College of Electrical Engineering and Information Engineering at Lanzhou University of Technology, Lanzhou, China. His research interests include image processing, image super-resolution and deep learning.

1 Introduction

Drought is a typical natural disaster with complex causes and difficult solutions, which has great influence on natural ecosystem, regional environment and social development. As the global climate climbs, the degree of global drought will also rise gradually (Huang et al., 2021). The Yellow River basin is an important agricultural production area in China, and the lower Yellow River is the main area of grain and cotton production. It can be said that the Yellow River basin plays a key role in promoting economic development and maintaining regional ecological stability (Zhou et al., 2019). Because of this, it is of

great significance to protect the ecological environment security of the Yellow River basin. However, the Yellow River basin is a drought-prone area, so it is of great practical significance to carry out drought monitoring projects in the Yellow River basin (Wang et al., 2019a).

In Zhang and Quan (2022), a drought monitoring method was designed based on Landsat time series image and nonlinear boundary information. In this method, time series images and land use/cover grid data are used as data sources to delete construction land information and water area information. Then, the LST-NDVI feature space was reconstructed by combining the mean value of the growing season with the seamless stitching technique. On this basis, the nonlinear fitting of dry boundary and wet boundary was carried out, and the spatial distribution grid of soil surface drought grade was obtained by inversion. In Cao et al. (2019), a monitoring method of drought spatial and temporal characteristics in the Yellow River basin based on combined drought index was designed. After collecting precipitation data, Gaussian Copula function and quasi-precipitation index were used to establish the combined drought index. On this basis, the temporal and spatial evolution characteristics of drought in the basin and the distribution of combined characteristics were analysed. In Deng et al. (2020), a watershed drought monitoring method based on GRACE gravity satellite data was designed. The method uses GRACE gravity satellites to collect relevant data in the study area, then performs dimensionless processing on the water storage deficit drought index, and compares it with the variation trend of the commonly used drought index to monitor the drought situation of the basin.

However, it is found that there is room for improvement in the accuracy of the extraction results of image boundary information and the fitting degree between drought monitoring results and actual results by the above traditional methods. To solve this problem, this study designed a drought monitoring method for the Yellow River basin based on boundary extraction of remote sensing images. The design ideas are as follows:

Step 1 By analysing the basic environmental situation of the Yellow River basin, it is found that the central area of the Yellow River basin is mostly loess landform, and the water and soil loss is relatively serious. Therefore, this study mainly focuses on the central area of the Yellow River basin, and designs the drought monitoring methods.

Step 2 Infrared, visible and panchromatic grey bands of ETM+ Landsat satellites were selected to collect real-time remote sensing images comprehensively to ensure the synchronisation of remote sensing images and geodesic data.

Step 3 The remote sensing image data is pre-processed by geometric correction and radiometric correction. Among them, radiometric calibration is used to complete radiometric correction, which can reduce the radiation error caused by illumination and atmospheric environment. Geometric correction is accomplished by correcting the geometric model and the projection of the field measurement control points of the image to avoid the influence of image deformation.

Step 4 The edge density and edge distribution are calculated according to the pre-processed remote sensing data. On the basis of reserving larger gradient edge points, the non-maximum suppression algorithm was used to suppress

edges in other gradient directions, and then the edge information of the region with the largest gradient change was used as the result to extract the edge information of remote sensing images.

Step 5 Relevant remote sensing indexes including hydrologic drought monitoring index, precipitation state index, land surface temperature state index and vegetation state index are calculated according to the boundary information, and the spatial inversion process of remote sensing index and land surface temperature characteristics is established. After elevation correction, drought monitoring level of the Yellow River basin is set, so as to complete drought monitoring.

2 Study area, data and methods

2.1 Overview analysis of the study area

The Yellow River basin spans the Qinghai-Tibet Plateau, Inner Mongolia Plateau, Loess Plateau and Huang-Huai-Hai plain from west to east. The western region is mountainous; in the central region, the altitude is between 1 km and 2 km, and most of them are loess landforms with serious soil erosion. The eastern part is mostly alluvial plain (Xu et al., 2021; Cheng et al., 2021).

The Yellow River basin merges with the sea in the east and lies inland in the west. Due to the large transverse span, the climate, precipitation, evaporation and other characteristics of different sections have great differences (Mohammadi et al., 2022).

2.2 Data acquisition

2.2.1 Obtaining remote sensing image data of the Yellow River basin

This study uses remote sensing mapping technology to obtain remote sensing image data of the Yellow River basin.

Table 1 Specific band information of ETM+ Landsat satellite

Serial number of bands	*Properties of bands*	*Resolving power*	*Wavelength*	*Attribute*
Band 1	Turquoise	0.46–0.53 m	30 μm	Visible light
Band 2	Green	0.53–0.61 m	30 μm	
Band 3	Red	0.64–0.70 m	30 μm	
Band 4	Near infrared	0.77–0.91 m	30 μm	Near infrared wave
Band 5	Mid infrared	1.56–1.76 m	30 μm	
Band 6	Thermal infrared	10.41–12.51 m	60 μm	Thermal infrared wave
Band 7	Mid infrared	2.10–2.36 m	30 μm	Near infrared wave
Band 8	Panchromatic micron	0.53–0.91 m	15 μm	

The remote sensing satellites used were ETM+ Landsat satellites. The satellite has high speed of information transmission and high resolution. Remote sensing images are

collected by infrared, visible and all grey bands of the satellite (Li et al., 2019). Specific band information is shown in Table 1.

Remote sensing image data of the Yellow River basin were obtained by using the above process, as shown in Figure 1.

Figure 1 Remote sensing image data of a section of Yellow River basin (see online version for colours)

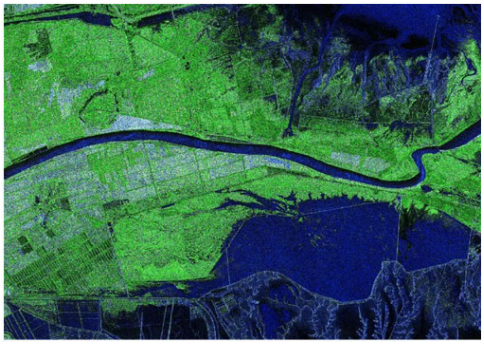

2.2.2 Remote sensing data pre-processing

Remote sensing image data is pre-processed by geometric correction and radiometric correction. Radiometric correction is divided into radiometric calibration and atmospheric correction. The absolute calibration method is used in the radiometric calibration. The atmospheric reflectance is obtained by data conversion, which can reduce the radiation error caused by light and atmospheric environment (Sourabh and Umesh, 2021; Kotaridis and Lazaridou, 2021). Atmospheric correction can reduce the radiation error caused by illumination and atmospheric environment so as to obtain accurate reflectance of ground objects (Yue et al., 2021).

First, calculate the emissivity, and the process is as follows:

$$\lambda = g \times L_\lambda \times DN_b + b \tag{1}$$

In formula (1), g represents the gain of the sensing acquisition process, L_λ represents the radiation brightness value, b represents the offset of remote sensing data coordinates, and DN_b represents DN value.

The emissivity is then converted into apparent outer atmospheric reflectance as follows:

$$\sigma = \frac{\pi \times \lambda \times d^2}{ESUN_\lambda \times \cos\theta} \tag{2}$$

In formula (2), d represents the distance between the earth and the sun, $ESUN_\lambda$ represents the average value of solar emissivity, and θ represents the angle between the direction of sunlight incident and the earth plane. The relevant calibration parameters are shown in Table 2.

The geometric correction process requires the collection of calibration model and field measurement point data, and the remote sensing image is projected onto the plane. The geometric correction model consists of triangular local area network module,

calculation module and transform image module, which can correct the geometric deformation, image and torsion.

Table 2 Scaling parameter

Bands	*θ*	$ESUN_\lambda$	*b*	*g*
1	52.39°	1,988	–6.987	0.797
2		1,823	–7.189	0.789
3		1,524	–5.612	0.632
4		1,040	–6.096	0.996
5		231.7	–1.162	0.162
6		84.82	–0.349	0.034

The correction process of triangular local network module and transform image module is as follows:

$$\begin{cases} x = F_x(u, v) = \sum_{i=0}^{N} \sum_{j=0}^{N-i} \beta u^i v^j \\ y = F_y(u, v) = \sum_{i=0}^{N} \sum_{j=0}^{N-i} \gamma u^i v^j \end{cases} \tag{3}$$

In formula (3), β and γ represent the image coefficient of transformation, N represents the order, u and v represent the image coordinates after transformation, F_x and F_y respectively represent the image before and after transformation, i represent the control point, and j represents the reference point.

The number of geometric correction is determined according to the number of control points, and the process is as follows:

$$n = \frac{(N+1)(N-1)}{2} \tag{4}$$

In formula (4), n represents the minimum number of control points. On this basis, the correction accuracy of control points is analysed and the correction is realised through adjustment, and the process is as follows:

$$RMS = \sqrt{(x'' - x')^2 + (y'' - y')^2} \tag{5}$$

In formula (5), x'' and y'' represent the corrected coordinates of the image control points, and x' and y' represent the ground coordinates of the control points.

When the following formula is satisfied, the geometric correction will achieve relatively high precision:

$$RMS \leq 1 \tag{6}$$

2.2.3 Remote sensing image boundary extraction

The edge of remote sensing image refers to the collection of pixels with uneven grey changes in the image and is an important feature of the image itself (Deeba et al., 2021). In this study, the edge density and edge distribution were calculated after the image data were pre-processed by geometric correction and radiometric correction.

When extracting the edge information of remote sensing image, the edge point set is firstly extracted by setting the threshold. The specific algorithm steps are as follows:

Step 1 Under the influence of complex remote sensing environment, there will inevitably be noise in remote sensing image. Noise information is mainly concentrated at high frequency signal, especially at the edge of image, which has a negative impact on the final target detection effect. Therefore, Gaussian filtering is firstly used to remove the noise information in the image, and the process is as follows:

$$W = H(x, y) \times \exp\left(-\frac{x^2 + y^2}{2\tau^2}\right) \tag{7}$$

In formula (7), $H(x, y)$ represents the Gaussian function and τ represents the smoothing parameter.

Step 2 Calculate the gradient of pixel points, and the calculation expression is:

$$\varphi(x, y) = \sqrt{(D(x, y+1) - D(x, y))^2 + (D(x+1, y) - D(x, y))^2} \tag{8}$$

In formula (8), D represents the gradient direction.

Step 3 In order to determine more accurate and clearer edge information, non-maximum suppression is performed on the edges obtained in the above steps. In this study, the size of edge points in different gradient directions is compared first, then the edge points with larger gradient are reserved, and the edges in other gradient directions are suppressed by non-maximum suppression algorithm. The edge information of the region with the largest gradient change was taken as the final extraction result, as shown in Figure 2.

Figure 2 Results of boundary extraction from remote sensing images of a region in the Yellow River basin (see online version for colours)

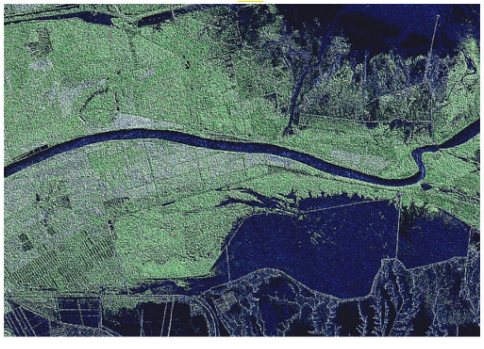

2.3 Design of drought monitoring method in Yellow River basin

Based on the above remote sensing image data of the Yellow River basin and boundary information extraction, relevant remote sensing indexes are calculated according to the boundary information, so as to design a specific drought monitoring method for the Yellow River basin.

Relevant remote sensing indices are as follows:

1 The hydrologic drought monitoring index can be used to indicate the degree to which water stocks deviate from normal hydrological conditions. The index is not affected by seasonal factors on land water storage (Wang et al., 2019b). Therefore, drought characteristics can be reflected more accurately, and the calculation process is as follows:

$$\mathrm{TWSD} = WSDI \times \epsilon + \delta \tag{9}$$

In formula (9), *WSDI* represents the water reserve deficit index, δ represents the standard deviation of water reserve deviation, and ϵ represents the average value of time series of water reserve deviation.

2 Precipitation state index is an index used to represent precipitation concentration, and its calculation process is as follows:

$$\mathrm{PCI} = \frac{p - p_{\min}}{p_{\max} - p_{\min}} \tag{10}$$

In formula (10), p represents the mean value of precipitation, $p_{\min}$ represents the lower line of precipitation, $p_{\max}$ represents the upper limit of precipitation.

3 Surface temperature state index. This indicator can reflect the temperature state of the surface. The calculation process of this indicator is as follows:

$$\mathrm{TCI} = \frac{t_{\max} - t}{t_{\max} - t_{\min}} \tag{11}$$

In formula (11), t represents the surface temperature at the collection time, $t_{\min}$ represents the downline of the surface temperature in the same period in history, and $t_{\max}$ represents the upper limit of the surface temperature in the same period in history.

4 Vegetation status index refers to the coverage degree of vegetation in a certain region. The calculation process of this index is as follows:

$$\mathrm{VCI} = \frac{v_i - v_{\min}}{v_{\max} - v_{\min}} \tag{12}$$

In formula (12), v_i represents the vegetation coverage in the i^{th} period of a characteristic year, $v_{\min}$ represents the minimum value of vegetation coverage in the simultaneous period, and $v_{\max}$ represents the maximum value of vegetation coverage in the simultaneous period.

On this basis, combined with the four remote sensing indices, the spatial inversion process of remote sensing index-LAND surface temperature characteristics is established, and its principle is shown in Figure 3.

Figure 3 Schematic diagram of spatial inversion process of remote sensing index – land surface temperature characteristics (see online version for colours)

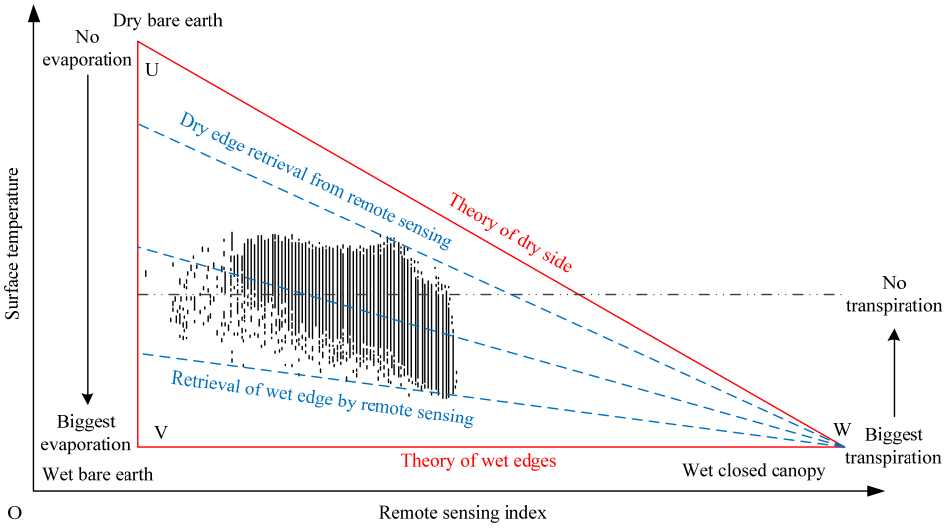

Observe Figure 1, in the triangle UVW, U represents dry bare soil, V represents wet bare soil, and W represents wet closed canopy. Oblique lines in feature space can be regarded as contour lines of surface temperature state index. The land surface temperature state index increases from bottom to top, and the land surface temperature state index with higher absolute slope value is more arid than the land surface temperature state index with lower absolute slope value. Therefore, relevant drought index can be determined by fitting the dry edge and wet edge of feature space.

Table 3 Drought monitoring grade setting table for Yellow River basin

Degree of drought	*Z*	*Remote sensing index*			
		TWSD	*PCI*	*TCI*	*VCI*
No drought	[0.90, 1.00]	45.1	74.2	91.8	60.2
Mild drought	[0.75, 0.90)	44.4	69.3	64.7	54.6
Moderate drought	[0.50, 0.75)	39.2	64.2	56.4	54.4
Severe drought	[0.35, 0.50)	36.6	50.0	28.9	26.9
Extreme drought	[0.00, 0.35)	18.6	43.6	21.8	16.7

As the surface of the Yellow River basin fluctuates greatly, the temperature difference is obvious, and the surface temperature is greatly affected by the elevation. Therefore, in order to improve the accuracy of monitoring the drought situation, it is necessary to further correct the elevation of the remote sensing index data. The process is as follows:

$$Z = (\mathrm{TWSD} + \mathrm{PCI} + \mathrm{TCI} + \mathrm{VCI}) = \alpha h \tag{13}$$

In formula (13), α represents the correction coefficient, which in this study is $\alpha = 0.006$, and h represents the elevation. According to the revised remote sensing index, the drought monitoring level of the Yellow River basin was set, and the results are shown in Table 3.

So far, according to the elevation correction results of remote sensing index data, the monitoring of drought in the Yellow River basin can be completed. The specific process is shown in Figure 4.

Figure 4 Flow chart of drought monitoring

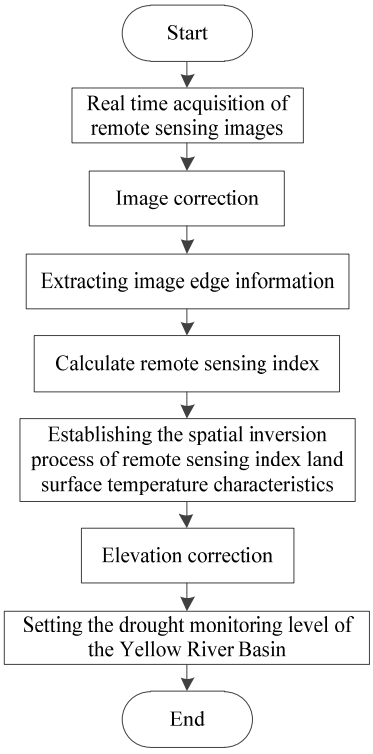

3 Experiments and results

3.1 Experiment design

In order to verify the practical application performance of the above designed drought monitoring method of the Yellow River basin based on boundary extraction of remote sensing images, the verification process is designed as follows.

The experiment was completed on the MATLAB simulation platform with Python as the development language, and the JetBrains PyCharm Community Edition compiler was used to process the relevant data. In the experiment, ETM+ Landsat satellite was used to collect real-time remote sensing images of the Yellow River basin. Satellite remote sensing bands are shown in Table 1.

In order to improve the experimental effect, a section in the middle of the Yellow River basin is selected as the test area, as shown in Figure 5.

Figure 5 The experimental section (see online version for colours)

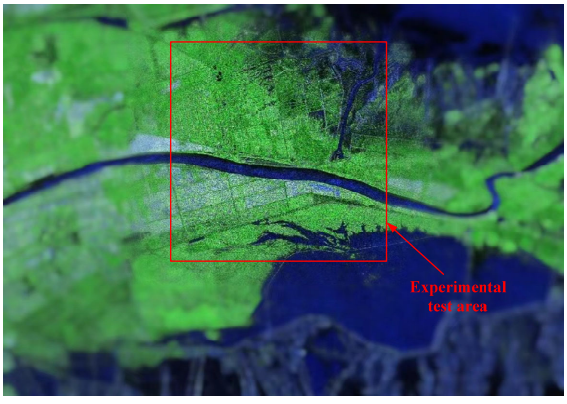

3.2 Contrast and index design

In order to improve the comparison of experimental results, the drought monitoring method based on Landsat temporal sequence image and nonlinear boundary information in Zhang and Quan (2022) and the drought spatial-temporal characteristics monitoring method based on combined drought index in Cao et al. (2019) were used as the comparison method.

In the experiment, the accuracy of image boundary information extraction and the degree of fitting between drought monitoring results and actual results were taken as indexes respectively to compare the application performance of different methods. The former can reflect the processing ability of different methods to remote sensing image information, while the latter can directly reflect the monitoring effect of different methods.

3.3 Results analysis

First, the accuracy of extracting results of image boundary information by different methods is tested, and the results are shown in Table 4.

Table 4 Comparison of accuracy of image boundary information extraction by different methods/%

Number of experiments	*Method of this paper*	*Method of Zhang and Quan (2022)*	*Method of Cao et al. (2019)*
2	96.2	91.3	87.2
4	97.4	90.5	86.3
6	94.3	90.8	86.1
8	93.5	91.1	84.7
10	91.7	90.5	82.9

By analysing the results shown in Table 4, it can be seen that with the continuous increase in the number of experiments, the accuracy of extraction results of image boundary information by method of Zhang and Quan (2022) is stable at 91% or so, and

the accuracy of extraction results by method of Cao et al. (2019) is continuously decreasing. Over the course of the experiment, its accuracy decreased from 87.2% to 82.9%. Although the accuracy of method of this paper's extraction results of image boundary information also showed a downward trend, its value always remained above 91.7%, indicating that method of this paper could collect remote sensing image information of the area to be monitored more accurately. The reason for this result is that this method calculates the edge density and edge distribution of the image after pre-processing the remote sensing data. Then, on the basis of retaining larger gradient edge points, the non-maximum suppression algorithm is used to suppress the edges in other gradient directions, and then the edge information of the area with the largest gradient change is taken as the result, so that the edge information of the remote sensing image can be extracted.

Then, the fitting degree between the drought monitoring results obtained by different methods and the actual results was tested, as shown in Figure 6.

Figure 6 Results of fitting degree between drought monitoring results and actual results (see online version for colours)

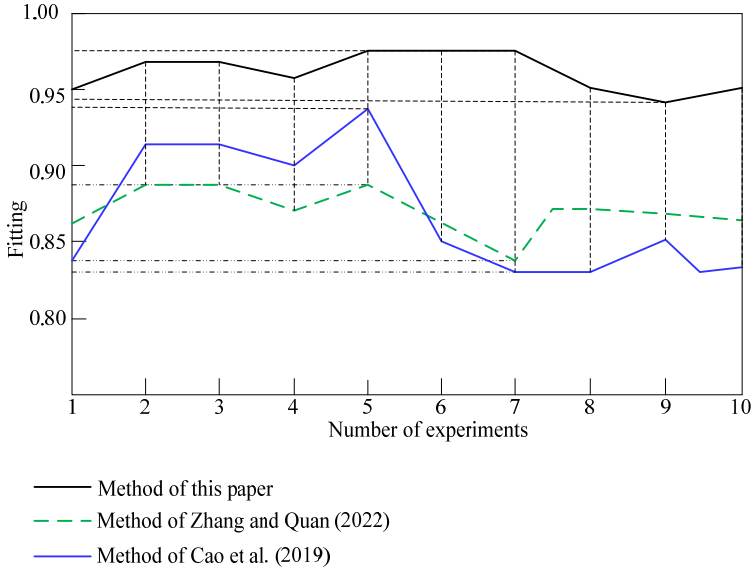

As shown in Figure 6, as the number of experiments continues to increase, the fitting degree of drought monitoring results obtained by different methods and actual results also keeps changing, and this change has no obvious rule. The fitting degree of method of Zhang and Quan (2022) and method of Cao et al. (2019) is between 0.95 and 0.80, while the fitting degree of method of this paper is always above 0.94. Method of this paper can more accurately monitor the drought situation in the Yellow River basin. The reason for this result is that this method calculates the hydrological drought monitoring index, precipitation state index, surface temperature state index and vegetation state index according to the boundary information, thus establishing the spatial inversion process of remote sensing index and surface temperature characteristics, and setting the drought

monitoring level of the Yellow River basin through elevation correction to improve the monitoring accuracy.

4 Conclusions

In view of the low accuracy and fit degree of traditional methods in regional drought monitoring, this study designed a drought monitoring method in the Yellow River basin based on boundary extraction of remote sensing images.

In this study, ETM+ Landsat satellite was selected to collect real-time remote sensing images comprehensively. By implementing geometric correction and radiometric correction for remote sensing image data, the radiometric errors caused by illumination conditions and atmosphere are eliminated, and the influence of image deformation is weakened. After the edge information of the image is extracted, the relevant remote sensing index is calculated according to the edge information, and the spatial inversion process of remote sensing index and surface temperature characteristics is established. The monitoring effect of drought in the Yellow River basin is improved through elevation correction.

According to the experimental results, the accuracy of this method for the extraction of image boundary information is high and its value always remains above 91.7%, and the fitting degree between the obtained drought monitoring results and the actual results is always above 0.94, indicating that this method can effectively realise the drought monitoring in the Yellow River basin.

Acknowledgements

This work was supported by the Henan Provincial Science and Technology Key Project Foundation under Grant No. 212102310085, No. 222102210142, No. 222102210252, and the key research project of colleges and universities in Henan province of China No. 23A520055, and the Henan Provincial Key Laboratory of Ecological Environment Protection and Restoration of the Yellow River basin Open Research Fund under Grant No. LYBEPR202202.

References

Cao, C., Ren, L., Liu, Y., Jiang, S., Zhang, L. and Zhang, L. (2019) 'Spatial temporal characteristics of drought of the Yellow River Basin based on joint drought index', *Yellow River*, Vol. 41, No. 5, pp.51–56.

Cheng, T., Hong, S., Huang, B., Qiu, J., Zhao, B. and Tan, C. (2021) 'Passive microwave remote sensing soil moisture data in agricultural drought monitoring: application in Northeastern China', *Water*, Vol. 13, No. 19, pp.2777–2792.

Deeba, F., Zhou, Y., Dharejo, F.A., Khan, M.A., Das, B., Wang, X. and Du, Y. (2021) 'A plexus-convolutional neural network framework for fast remote sensing image super-resolution in wavelet domain', *IET Image Processing*, Vol. 15, No. 8, pp.1679–1687.

Deng, Z., Wu, X., Wang, Z., Li, J. and Chen, X. (2020) 'Drought monitoring based on GRACE data in the Pearl River Basin, China', *Transactions of the Chinese Society of Agricultural Engineering*, Vol. 36, No. 20, pp.179–187.

Huang, T., Lin, Q., Wu, Z. and Wang, Y. (2021) 'Spatial and temporal characteristics of drought in the Yellow River Basin and their correlation with ENSO', *Yellow River*, Vol. 43, No. 11, pp.52–58.

Kotaridis, I. and Lazaridou, M. (2021) 'Remote sensing image segmentation advances: a meta-analysis', *ISPRS Journal of Photogrammetry and Remote Sensing*, Vol. 173, No. 1, pp.309–322.

Li, Y., Ning, S., Ding, W., Jin, J. and Zhang, Z. (2019) 'The evaluation of latest GPM-era precipitation data in Yellow River Basin', *Remote Sensing For Land & Resources*, Vol. 31, No. 1, pp.164–170.

Mohammadi, N., Sedaghat, A. and Mahya, J.R. (2022) 'Rotation-invariant self-similarity descriptor for multi-temporal remote sensing image registration', *The Photogrammetric Record*, Vol. 37, No. 177, pp.6–34.

Sourabh, P. and Umesh, P.C. (2021) 'A comprehensive review on remote sensing image registration', *International Journal of Remote Sensing*, Vol. 42, No. 14, pp.5400–5436.

Wang, L., Huang, S., Huang, Q., Fang, W., Li, K. and Zhang, Y. (2019a) 'Drought multivariable probability characteristics based on a multivariate standardized drought index in the Yellow River basin', *Journal of Natural Disasters*, Vol. 28, No. 6, pp.70–80.

Wang, Y., Shang, W. and Peng, S. (2019b) 'Yellow River basin drought response system based on the prediction and operation of cascade reservoirs', *Advances in Water Science*, Vol. 30, No. 2, pp.175–185.

Xu, Z., Wu, Z., He, H., Guo, X. and Zhang, Y. (2021) 'Comparison of soil moisture at different depths for drought monitoring based on improved soil moisture anomaly percentage index', *Water Science and Engineering*, Vol. 14, No. 3, pp.171–183.

Yue, H., Liu, Y. and Qian, J. (2021) 'Comparative assessment of drought monitoring index susceptibility using geospatial techniques', *Environmental Science and Pollution Research*, Vol. 28, No. 29, pp.1–21.

Zhang, X. and Quan, Q. (2022) 'Soil drought monitoring based on Landsat time-series images and nonlinear edges: a case study of the growing season in Inner Mongolia section of the Yellow River from 1986 to 2020', *Hydro-Science and Engineering*, Vol. 36, No. 2, pp.126–134.

Zhou, S., Wang, Y., Chang, J., Guo, A. and Li, Z. (2019) 'Research on spatio-temporal evolution of drought patterns in the Yellow River Basin', *Journal of Hydraulic Engineering*, Vol. 50, No. 10, pp.1231–1241.